

POR

EGG-NTAP-6309

September 1983

ANALYSIS OF THE JUNE 24, 1980 LOSS OF OFF-SITE  
POWER TRANSIENT AT ARKANSAS NUCLEAR ONE UNIT 2

Paul D. Bayless

**Idaho National Engineering Laboratory**

Operated by the U.S. Department of Energy



This is an informal report intended for use as a preliminary or working document

Prepared for the  
U.S. NUCLEAR REGULATORY COMMISSION  
Under DOE Contract No. DE-AC07-76ID01570  
FIN No. A6234

8403280117 830930  
PDR ADOCK 05000368  
S PDR

50-368  
 **EG&G** Idaho

ANALYSIS OF THE JUNE 24, 1980 LOSS OF OFF-SITE POWER TRANSIENT  
AT ARKANSAS NUCLEAR ONE UNIT 2

Paul D. Bayless

Published September 1983

EG&G Idaho, Inc.  
Idaho Falls, Idaho 83415

Prepared for the  
U.S. Nuclear Regulatory Commission  
Washington, D.C. 20555  
Under DOE Contract No. DE-AC07-76ID01570  
FIN No. A6234

### ABSTRACT

The June 24, 1980 loss of off-site power transient at Arkansas Nuclear One Unit 2 was analyzed using the RELAP5 computer code. The transient was investigated to understand the overall plant response, particularly in relation to natural circulation cooling. Sensitivity calculations were performed to identify operator actions that may have been taken during the transient. The effect of the various sensitivity calculations on natural circulation was examined. Methods of identifying the presence of natural circulation cooling were investigated.

FIN No. A6234--Analytical Assessment of Reactor Operational Events

## SUMMARY

An analysis of the June 24, 1980 loss of off-site power (LOSP) transient at Arkansas Nuclear One Unit 2 (ANO-2) was performed using the RELAP5 computer code. The analysis of the LOSP transient was performed by EG&G Idaho, Inc., at the Idaho National Engineering Laboratory. This analysis was the first in a series of analyses requested by the Nuclear Regulatory Commission Office for Analysis and Evaluation of Operational Data to support case studies of natural circulation events in pressurized water reactors (PWRs). ANO-2 is a Combustion Engineering PWR with a rated core thermal power of 2815 MW. RELAP5 is an advanced computer code designed for one-dimensional, thermal-hydraulic analysis of nuclear reactor and related experimental systems.

The analysis was performed to provide an understanding of the overall plant response, with emphasis on natural circulation cooling. It was also intended to identify operator actions that may have been taken during the transient and to investigate their effect on natural circulation.

Sensitivity studies were performed on various boundary conditions to determine what may have caused the measured plant response. Most of these studies involved the secondary coolant system. In a natural circulation situation, the response of the reactor coolant system is sensitive to the secondary system pressure. The reactor coolant system response was also found to be sensitive to the pump coastdown.

From the analysis, it was concluded that atmospheric dump valves were opened to depressurize the secondary coolant system, then were closed. It was also concluded that the chemical and volume control system was controlled manually to increase the pressurizer liquid level above the setpoint level.



The transition to and presence of natural circulation cooling could be inferred from temperature measurements. The cold leg temperature was closely coupled to the steam generator temperature during natural circulation. Also, the difference between the hot and cold leg temperatures increased during the transition from forced convection to natural circulation cooling, then stayed fairly constant in fully developed natural circulation flow. The flow rate and loop temperature difference in fully developed natural circulation were determined by the core power and loop flow resistance.

## CONTENTS

ABSTRACT .....	ii
SUMMARY .....	iii
1. INTRODUCTION .....	1
2. MODEL DESCRIPTION .....	3
2.1 Nodalization .....	3
2.2 Initial Conditions .....	10
2.3 Boundary Conditions .....	10
3. TRANSIENT ANALYSIS .....	13
3.1 Transient Investigation .....	13
3.2 Natural Circulation .....	27
4. CONCLUSIONS .....	36
5. REFERENCES .....	38

## FIGURES

1. RELAP5 nodalization of ANO-2 coolant loops .....	4
2. RELAP5 nodalization of ANO-2 reactor vessel .....	5
3. RELAP5 nodalization of ANO-2 A steam generator .....	6
4. RELAP5 nodalization of ANO-2 B steam generator .....	7
5. RELAP5 nodalization of ANO-2 A main steam line .....	8
6. RELAP5 nodalization of ANO-2 B main steam line .....	9
7. Pressurizer pressure from the base case and the plant data .....	14
8. Pressurizer liquid level from the base case and the plant data .....	14
9. Hot leg temperature from the base case and the plant data .....	15

10.	Cold leg temperature from the base case and the plant data .....	15
11.	Steam generator A pressure from the base case and the plant data .....	16
12.	Steam generator A narrow range liquid level from the base case and the plant data .....	16
13.	Steam generator A pressure from the SDBCS case, the base case, and the plant data .....	20
14.	Steam generator A pressure from the 3% dump flow case, the 10% dump flow case, and the plant data .....	20
15.	Pressurizer pressure from the controlled pressure case, the base case, and the plant data .....	22
16.	Pressurizer liquid level from the controlled pressure case, the base case, and the plant data .....	22
17.	Steam generator A pressure from the controlled pressure case, the base case, and the plant data .....	23
18.	Steam generator A narrow range liquid level from the controlled pressure case, the base case, and the plant data .....	23
19.	Hot leg temperature from the controlled pressure case, the base case, and the plant data .....	24
20.	Cold leg temperature from the controlled pressure case, the base case, and the plant data .....	24
21.	Loop average temperature from the controlled pressure case, the base case, and the plant data .....	25
22.	Hot leg mass flow rate from the pump friction case and the controlled pressure case .....	28
23.	Loop average temperature from the pump friction case, the controlled pressure case, and the plant data .....	28
24.	Pressurizer pressure from the pump friction case, the controlled pressure case, and the plant data .....	29
25.	Pressurizer liquid level from the pump friction case, the controlled pressure case, and the plant data .....	29
26.	Hot leg mass flow rate from the base case, the controlled pressure case, the SDBCS case, and the pump friction case .....	31

27.	Cold leg and steam generator temperatures from the controlled pressure case .....	31
28.	Cold leg and steam generator temperatures from the plant data ....	32
29.	Loop temperature difference from the base case, the controlled pressure case, and the plant data .....	32
30.	Loop temperature difference from the pump friction case, the SDBCS case, the base case, the controlled pressure case, and the plant data .....	34

## TABLE

1.	Initial Conditions .....	11
----	--------------------------	----

## 1. INTRODUCTION

The loss of off-site power (LOSP) transient that occurred at Arkansas Nuclear One Unit 2 (ANO-2) on June 24, 1980 was analyzed. The principal analysis tool used was the RELAP5 computer code. The analysis was performed in support of pressurized water reactor (PWR) natural circulation case studies being performed by the Nuclear Regulatory Commission Office for Analysis and Evaluation of Operational Data. This is the first in a series of reports on natural circulation events.

ANO-2 is a Combustion Engineering PWR with a rated core power of 2815 MW(t). On June 24, 1980 it was operating at 91% power when a partial LOSP occurred, resulting in a temporary loss of all AC power to the plant. The diesel generators started automatically, as did the emergency feedwater (EFW) pumps. These were the only actions affecting the primary system known to have taken place prior to the restarting of the reactor coolant pumps.

The objectives of this analysis were to understand the plant response during the transient, to identify possible operator actions that would account for the plant response, and to investigate natural circulation phenomena. Since the primary interest was in natural circulation, only the first 900 s of the transient was investigated. The reactor coolant pumps coasted down and natural circulation was established in this time period.

RELAP5/MOD1.5<sup>1</sup> is an advanced computer code designed for best estimate thermal-hydraulic analysis of postulated light water reactor transients. It is a one-dimensional analysis code based on a nonhomogeneous, nonequilibrium hydrodynamic model that utilizes one energy, two momentum, and two continuity equations. The versions of the code used in this analysis were cycles 27 and 30, which have been stored under Configuration Control Numbers F01137 and F01187, respectively, at the Computer Science Laboratory at the Idaho National Engineering Laboratory.

The data presented in this report were digitized from strip charts and other plots from data that were recorded during the transient and presented in the preliminary unit transient report.<sup>2</sup> The quality of the measured data was not known. Some of the strip charts had noticeable offsets, so the data trends were considered more important than the magnitudes. The uncertainties in the time scales of the data presented in this report were estimated to be  $\leq 5$  s for the first 275 s, and  $\leq 100$  s thereafter. The dual data traces (after 275 s) in the plots of the pressurizer pressure and hot leg temperature show the values recorded by redundant measurements.

A description of the RELAP5 model of ANO-2, including the initial and boundary conditions, is presented in Section 2. Results of the analysis of the LOSP transient are presented in Section 3. Conclusions drawn from the analysis are presented in Section 4. References are presented in Section 5.



## 2. MODEL DESCRIPTION

The RELAP5 nodalization of ANO-2 used in the analysis is described in Section 2.1. The initial conditions are described in Section 2.2, and the boundary conditions are discussed in Section 2.3.

### 2.1 Nodalization

The RELAP5 model of ANO-2 consisted of 201 volumes, 208 junctions, and 168 heat structures. Nodalization diagrams for various parts of the plant are presented in Figures 1 through 6. The hydrodynamic components were modeled to represent the actual flow areas, lengths, volumes, and elevation changes that exist in the plant. The heat structures were modeled to represent the actual stored energy and heat transfer area of the metal components of the plant.

The nodalization of the coolant loops is shown in Figure 1. Both loops in the plant were modeled with each containing one hot leg, one steam generator, two cold legs, and two reactor coolant pumps. The pressurizer was connected to the A loop hot leg. The pressurizer model included the heaters, the surge line, and the main spray line. Charging flow was injected into one cold leg in each loop, and letdown was taken from one of the pump suction legs. Control systems were provided to operate the charging, letdown, and pressurizer heaters as they are operated in the plant. The charging and letdown were controlled by the deviation from the pressurizer setpoint level, which was determined by the loop average temperature. The proportional heater power varied linearly from full power at 15.34 MPa (2225 psia) to zero at 15.69 MPa (2275 psia).

The nodalization of the reactor vessel is shown in Figure 2. The reactor vessel was modeled to include the downcomer, lower plenum, core, upper plenum, upper head, core bypass flow paths, internals, and fuel rods. The modeled core bypass flow paths included the outlet nozzle clearances, the alignment key-ways, the support cylinder holes, the core shroud clearances, and the guide tubes. The outlet nozzle clearance and alignment key-ways paths were lumped together and connected the inlet

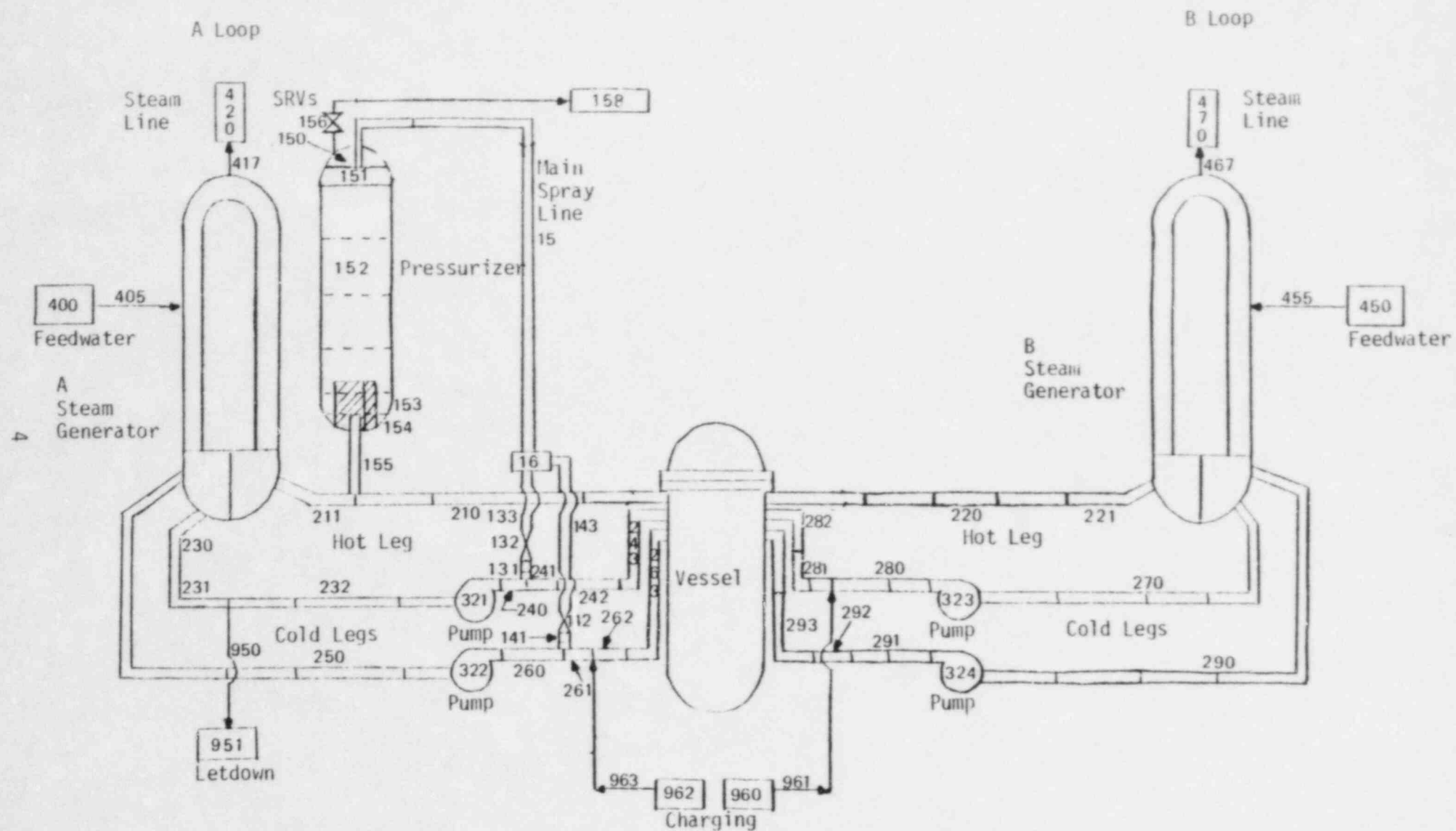


Figure 1. RELAP5 nodalization of ANO-2 coolant loops.

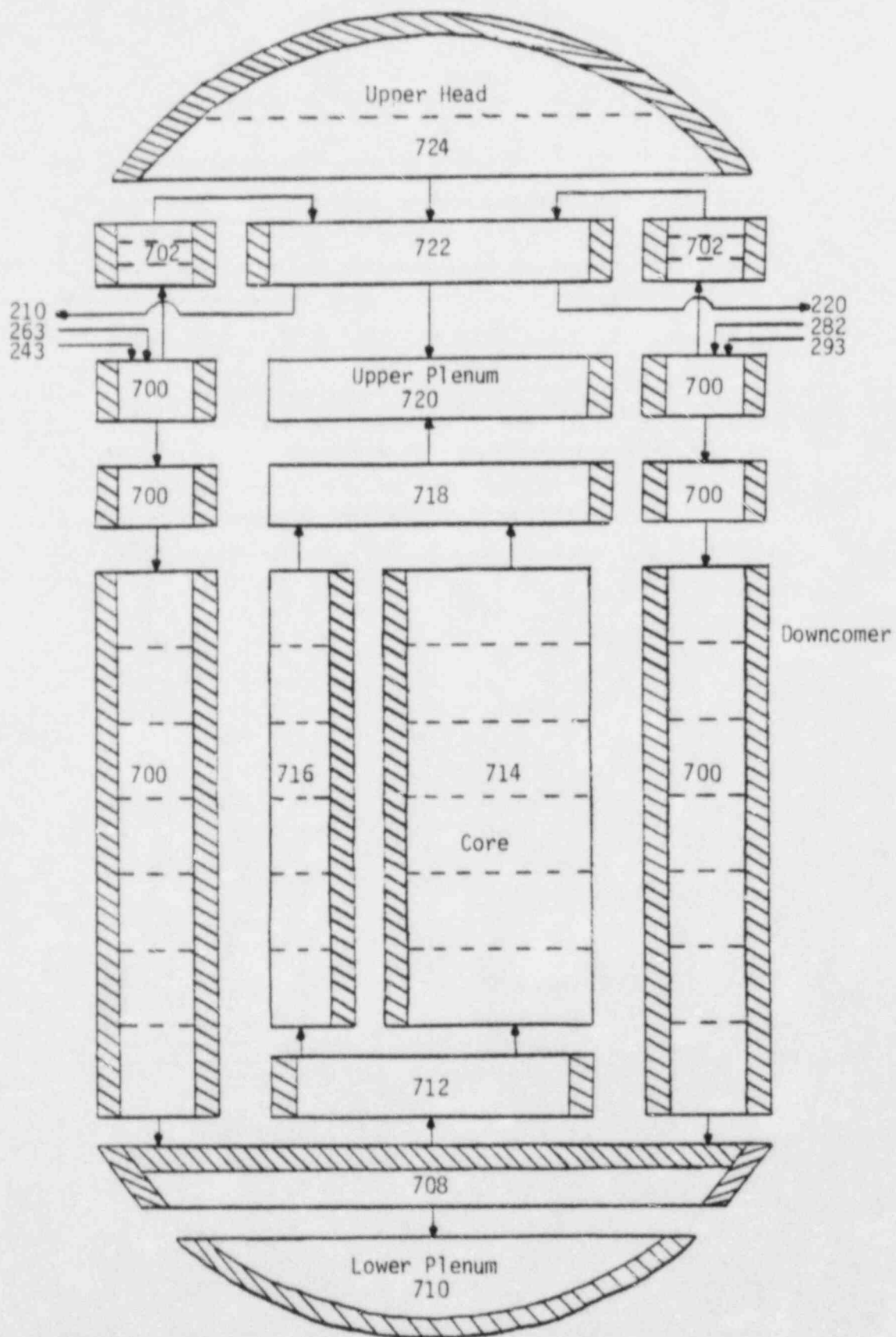


Figure 2. RELAP5 nodalization of ANO-2 reactor vessel.

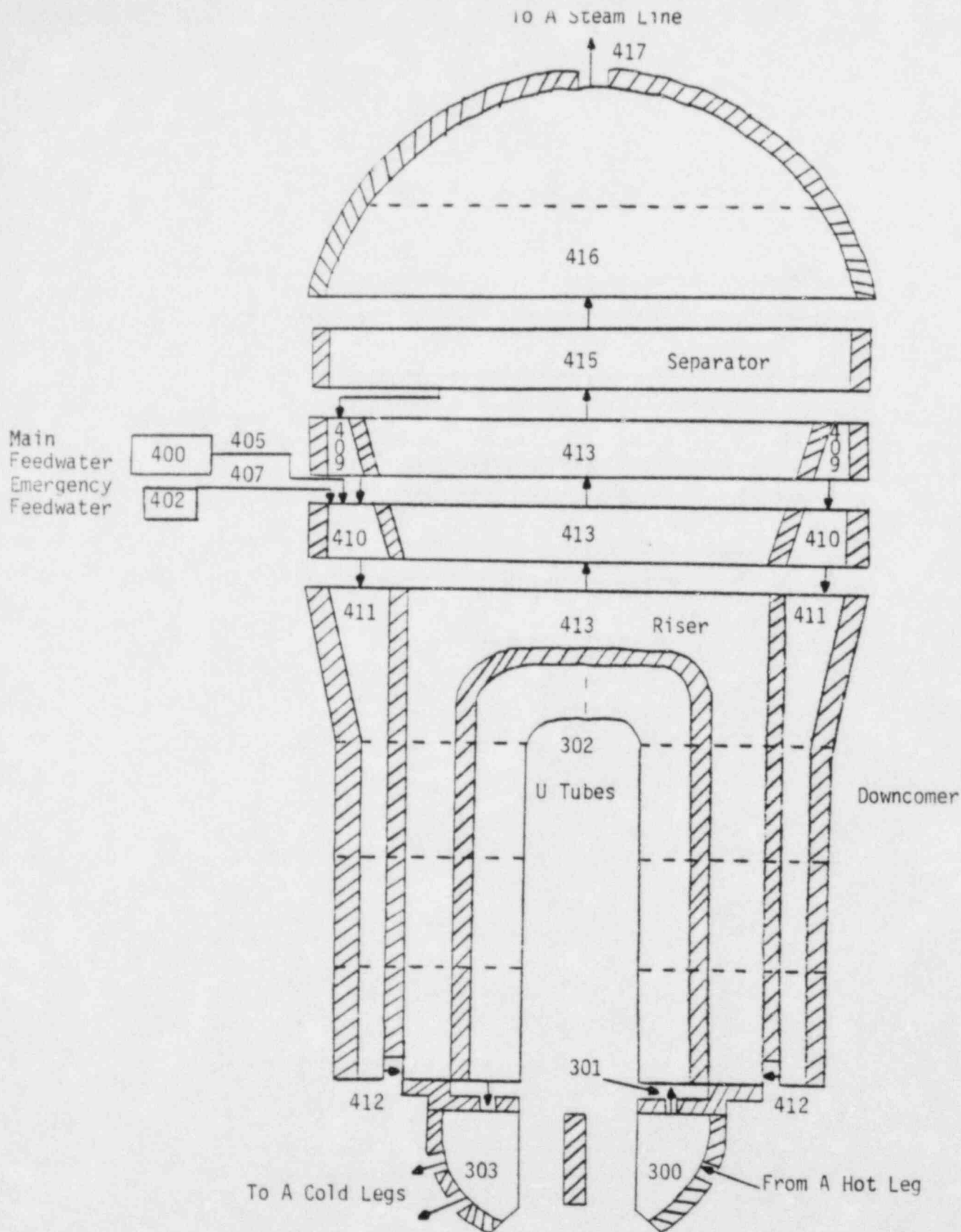


Figure 3. RELAP5 nodalization of ANO-2 A steam generator.

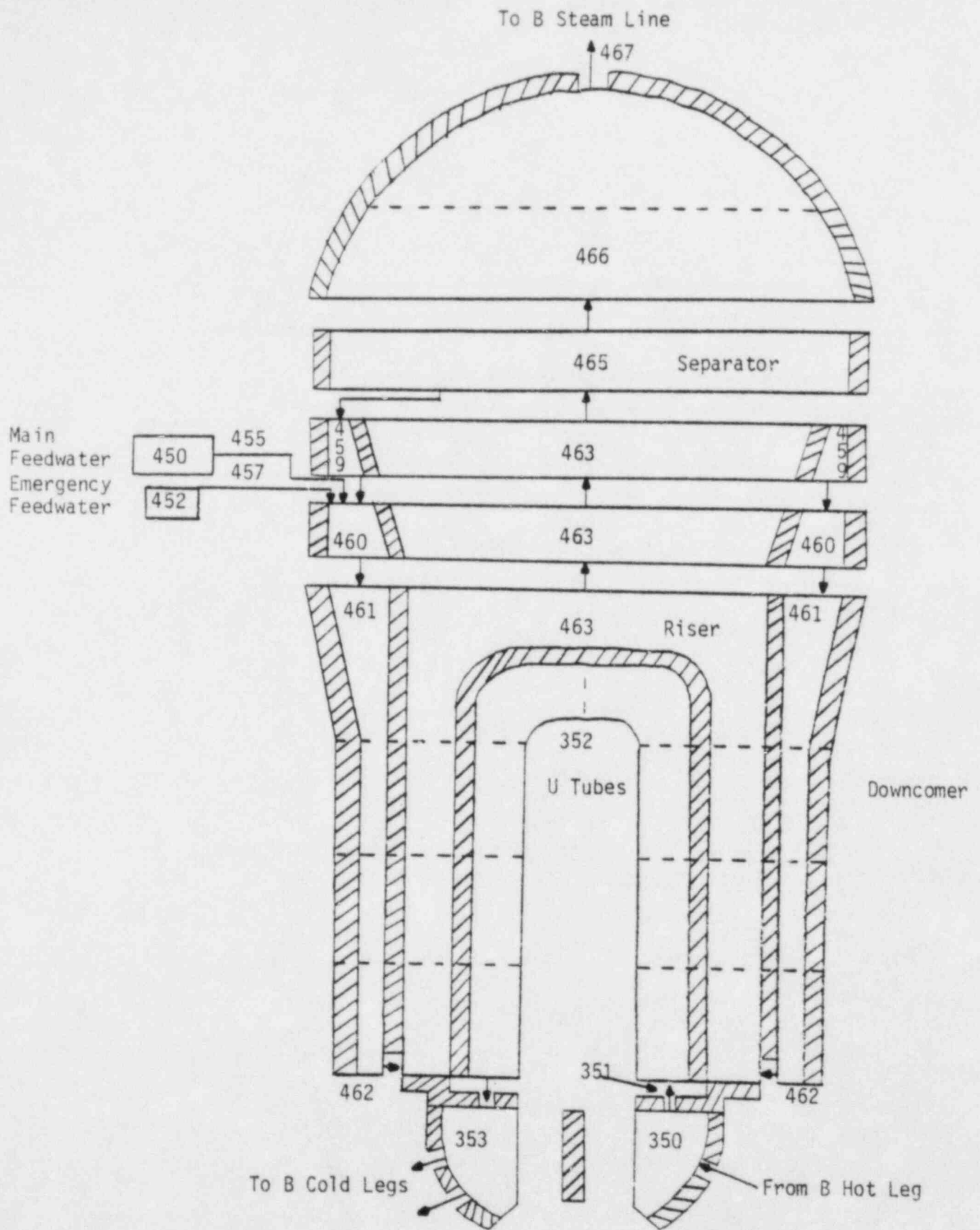


Figure 4. RELAP5 nodalization of ANO-2 B steam generator.

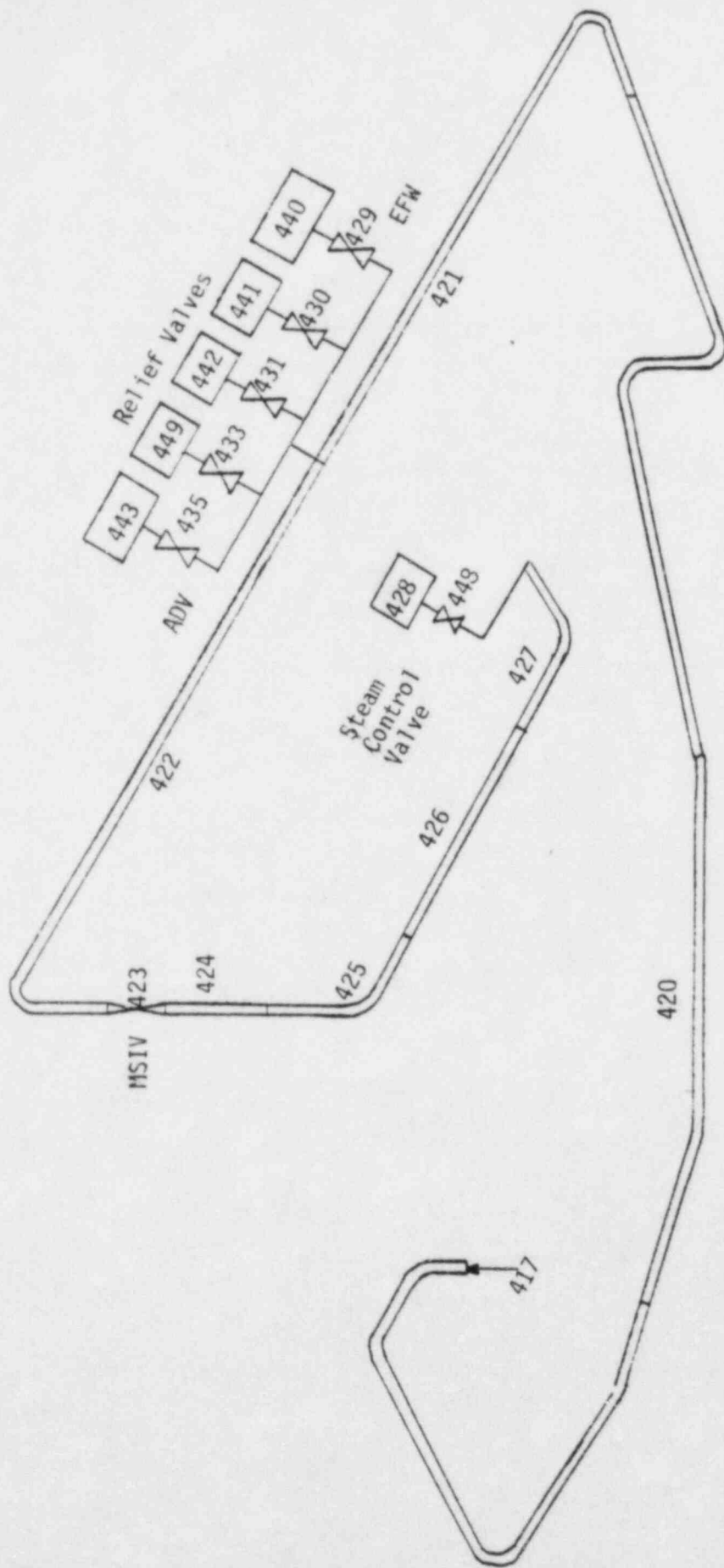


Figure 5. RELAP5 nodalization of ANO-2 A main steam line.



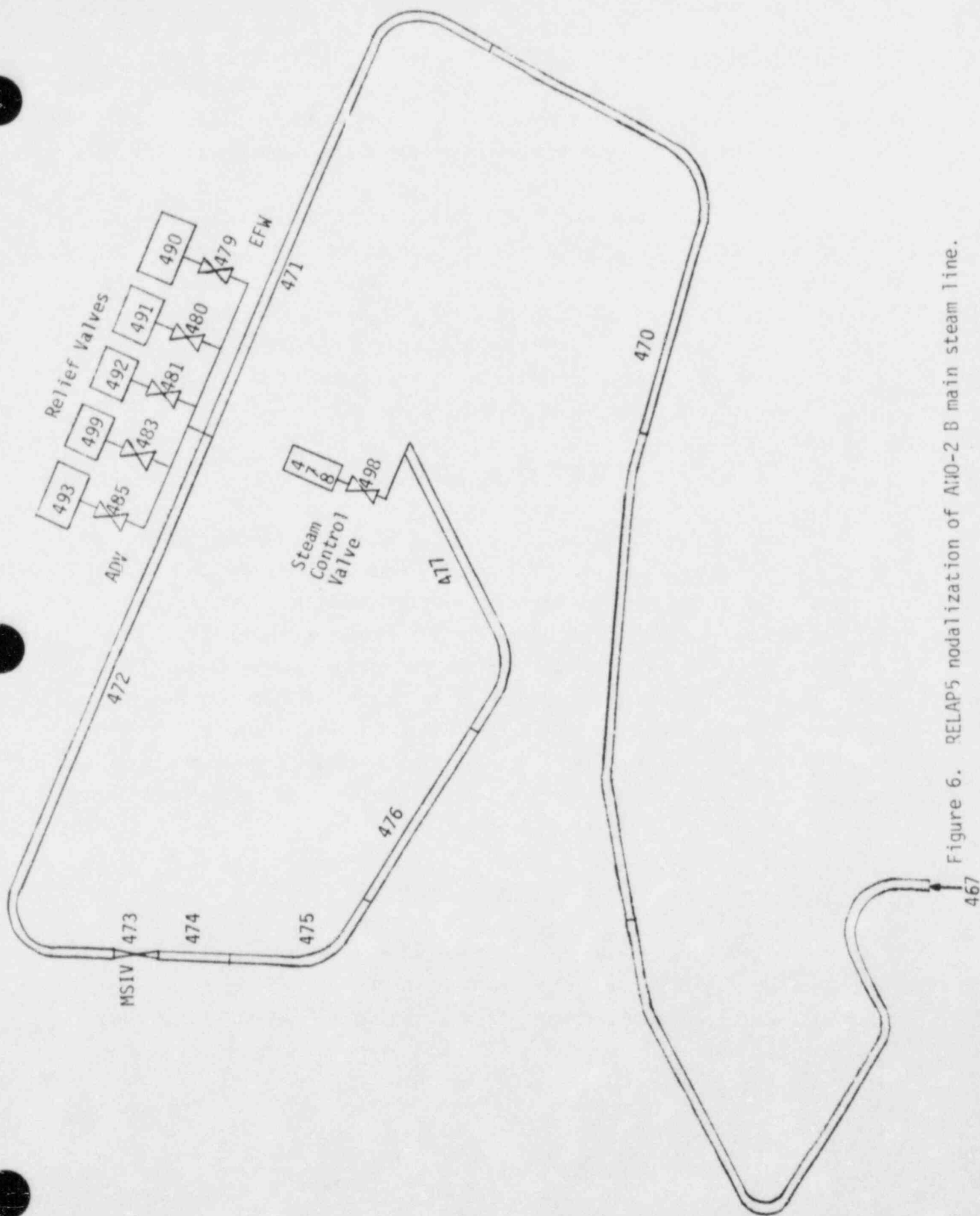


Figure 6. RELAP5 nodalization of A10-2 B main steam line.

annulus to the upper plenum. The support cylinder holes, core shroud clearance paths and guide tubes were lumped together as a flow path parallel to but separate from the core. The portion of the guide tube bypass from the lower plenum to the upper head was not modeled explicitly.

Figures 3 through 6 present the nodalization of the secondary coolant system. The main and emergency feedwater connections to the steam generators were modeled. The main steam lines were modeled from the steam generators to the main steam control valves. Several connections to each steam line upstream of the main steam isolation valves (MSIVs) were also modeled: five relief valves (lumped into three valves), one atmospheric dump valve, and the steam supply to the EFW pump turbine.

## 2.2 Initial Conditions

The initial conditions used in the RELAP5 calculations are compared to the actual transient initial conditions in Table 1. The plant initial conditions were obtained from strip charts and computer printouts. The RELAP5 initial values were obtained from a steady state calculation in which the reactor coolant pumps, chemical and volume control system (CVCS), and feedwater and steam flows were operated by control systems. The agreement between the calculated and actual values was generally excellent. Differences in the reactor coolant flow and the steam generator level could have been caused by how these parameters were controlled in the calculation and by uncertainties in the measured data.

## 2.3 Boundary Conditions

The boundary conditions described below are those that were assumed for the RELAP5 calculations. At transient initiation, the reactor was scrammed, main feedwater was shut off, and the MSIVs began to close. The charging pumps were stopped, and the letdown valve was held in its steady state position.

TABLE 1. INITIAL CONDITIONS

Parameter	RELAP5	Plant
Core power, %	91	91
Pressurizer pressure, MPa (psia)	15.44 (2240)	15.44 (2240)
Hot leg temperature, K (°F)	592.4 (606.7)	593 (607)
Cold leg temperature, K (°F)	562.4 (552.7)	562 (552)
Pressurizer level, %	49	49
Reactor coolant flow, kg/s (lbm/s)	15,300 (33,700)	16,900 (37,200)
Charging flow, l/s (gpm)	2.78 (44.0)	unavailable
Letdown flow, l/s (gpm)	2.74 (43.5)	unavailable
Steam generator pressure, MPa (psia)	6.34 (920)	6.14 (890)
Steam generator narrow range liquid level, %	89	74
Steam flow, kg/s (lbm/s)	720 (1590)	730 (1600)
Feedwater flow, kg/s (lbm/s)	720 (1590)	730 (1600)

At 0.8 s, the reactor coolant pumps were tripped.<sup>a</sup> The MSIVs were closed at 3.0 s. Power from the diesel generators was available beginning at 14.3 s.<sup>a</sup> The letdown valve returned to automatic operation at this time. At 16.3 s, the charging pumps were available and the turbine-driven EFW pump started. The motor-driven EFW pump started 20 s after the diesel generators were available. Each EFW pump provided 36.3 l/s (575 gpm) of 303 K (85°F) water. Power to 300 kW of proportional pressurizer heaters was available at 104.3 s. The loading sequence for the diesel generators was obtained from the final safety analysis report.<sup>3</sup>

The decay power was calculated using a separate effects RELAP5 model, and was based on 100 full power days of operation prior to the scram.

In nearly all the calculations, the pressurizer level setpoint was changed to 50%, regardless of the average temperature, to reflect Combustion Engineering guidelines for operators following a LOSP.

---

a. Event time obtained from Reference 2.

### 3. TRANSIENT ANALYSIS

Results of the evaluation of the plant thermal-hydraulic response during the transient are presented in Section 3.1. An analysis of how the various conditions simulated in the sensitivity studies affected natural circulation and of how natural circulation might be identified is presented in Section 3.2.

#### 3.1 Transient Investigation

From the information available in Reference 2, the relative timing of the reactor scram, reactor coolant pump trip, and diesel generator startup was known. It was also known that both EFW pumps started automatically. No other actions affecting the boundary conditions were mentioned. The strip chart of the pressurizer liquid level and setpoint level, however, showed that the measured level surpassed the setpoint at about 500 s. This indicates that the operators were manually controlling the CVCS by 500 s. No further insight into other boundary conditions that might have been affected could be gained from Reference 2 alone.

A base calculation was performed using only the boundary conditions described in Section 2.3. Major parameters from this calculation are compared with the plant data in Figures 7 through 12.

Figure 7 presents the pressurizer pressure comparison. The rapid initial depressurization was caused by the coolant shrink following the reactor scram. The liquid in the reactor coolant system became more dense as it cooled, thus shrinking the volume occupied by liquid, which increased the steam volume and lowered the pressure. The pressure increase between 50 and 300 s was caused by an increase in the average temperature that was caused by the transition to natural circulation cooling. The temperature response will be discussed in more detail later. The pressure increase after 350 s was caused by the CVCS filling the system and the power input from the pressurizer heaters. The oscillations in the

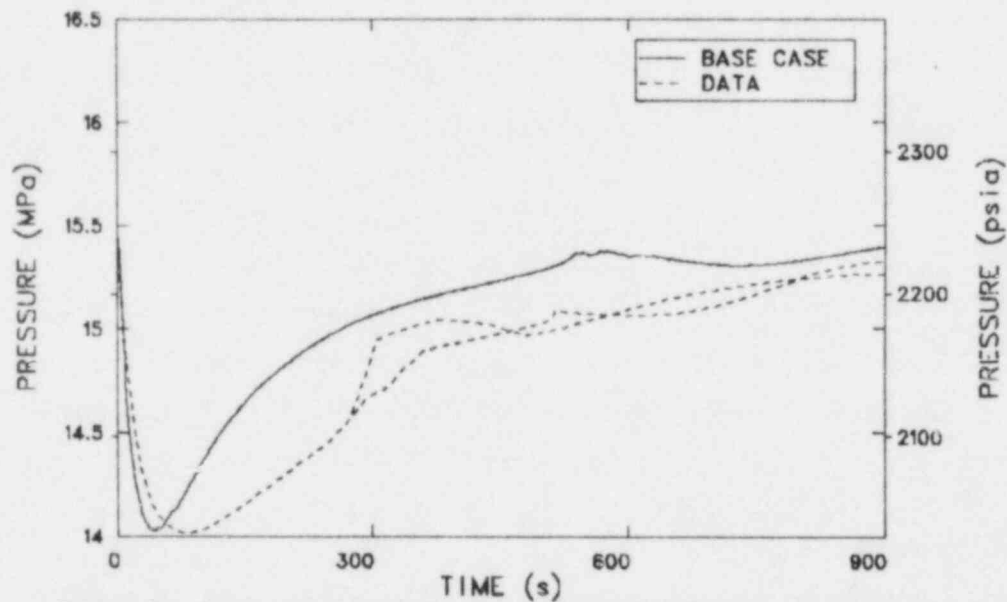


Figure 7. Pressurizer pressure from the base case and the plant data.

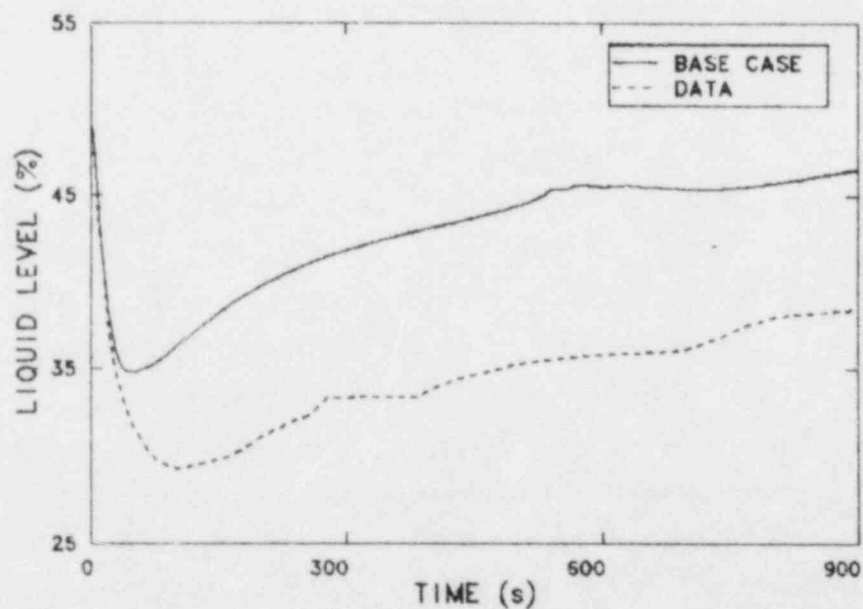
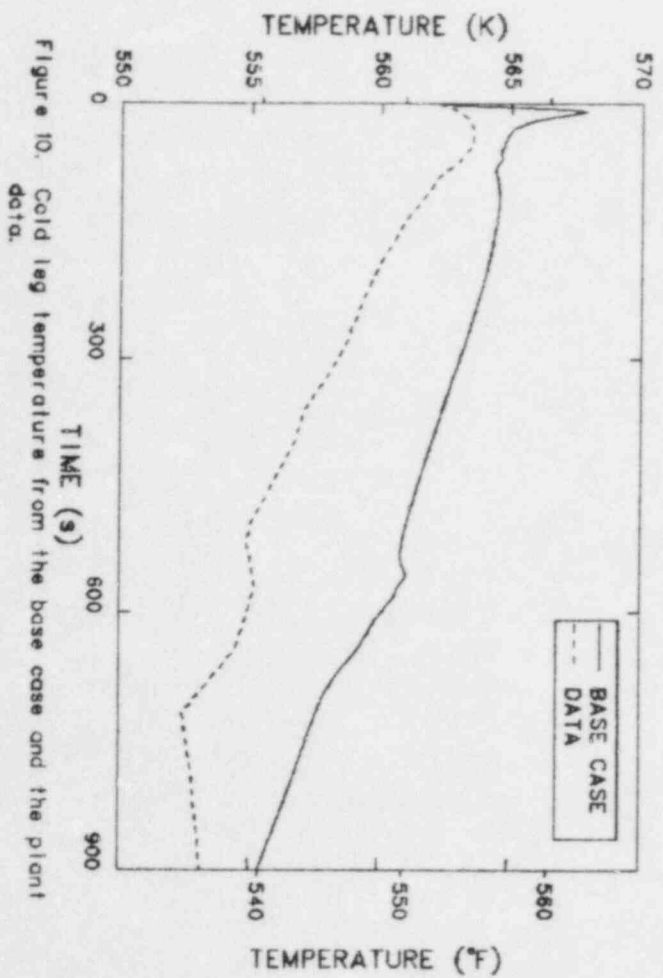
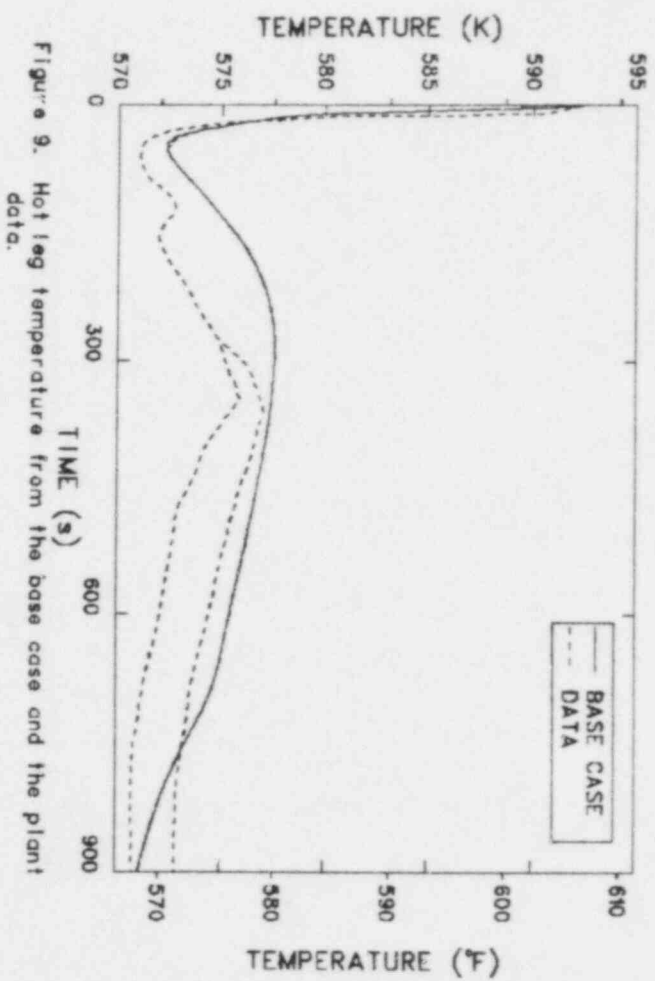


Figure 8. Pressurizer liquid level from the base case and the plant data.





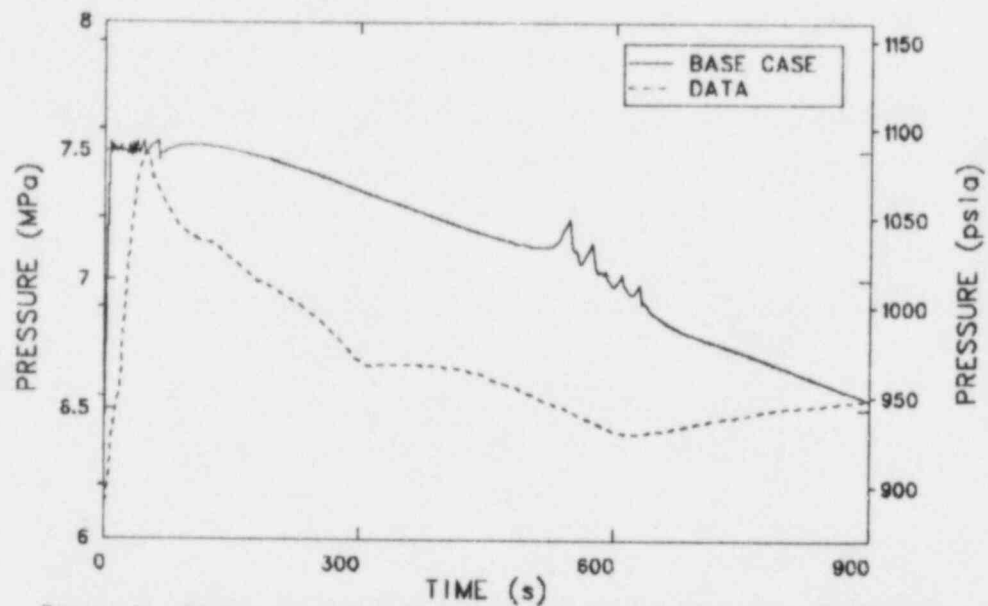


Figure 11. Steam generator A pressure from the base case and the plant data.

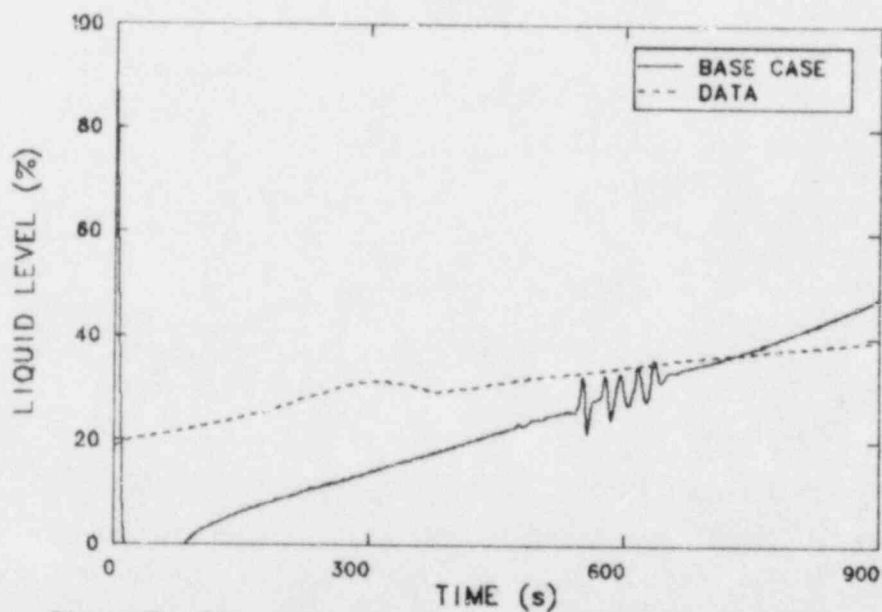


Figure 12. Steam generator A narrow range liquid level from the base case and the plant data.

calculated pressure between 500 and 650 s were related to a transition in the condensation model in RELAP5, and did not reflect a realistic pressure behavior.

The pressurizer level comparison is shown in Figure 8. The rapid level decrease was the result of the post-scam shrink. The level increase between 50 and 300 s was caused by the coolant heatup, and the gradual increase through the rest of the transient reflected the liquid injection by the CVCS.

Figure 9 presents the hot leg temperature comparison. The temperature decreased sharply in the first 50 s as the core power was reduced after scam and the flow was still relatively high. As the pumps coasted down, the flow was decreasing faster than the power, so the liquid passing through the core was heated more, and the temperature increased. The temperature then decreased after about 300 s as natural circulation flow was fully established and the power slowly decreased.

The cold leg temperatures are compared in Figure 10. The increase in temperature in the first 20 s was caused by a reduced heat transfer rate to the secondary coolant system. The steam generators were isolated (no feedwater, MSIVs closed), increasing their pressures (and temperatures) and reducing the temperature difference across the steam generator tubes. The pumps were coasting down, which reduced the heat transfer coefficient on the primary side of the tubes. These factors combined to reduce the heat transferred from the liquid as it passed through the steam generator. The temperature then decreased as the steam generator pressure decreased and the core power decayed. The slight temperature increase in the data beginning at approximately 700 s was caused by increasing pressure in the steam generator secondary side.

The steam generator pressures are compared in Figure 11. The pressure increased as the MSIVs were closed and heat continued to be transferred from the reactor coolant system. The lowest pressure steam line relief valves opened at about 5 s. In the calculation, the pressure slowly decreased after 100 s as the EFW was able to condense more steam than the

heat transferred from the reactor coolant system could create. The oscillations between 500 and 650 s were caused by the condensation rate transition in the code, and were not realistic. The slower pressure increase in the plant data during the first 50 s indicated that more steam may have been vented in the early stages of the transient than was assumed in the calculation. The more rapid pressure decrease in the plant data after 50 s indicated that steam may have been released by other means in addition to the relief valves. The leveling off of the pressure near 300 s and the pressure increase beginning at about 600s could have been caused by changes in the steam flow or EFW flow. It is important to note that the slope changes in the measured data at 50, 300, and 600 s were not observed in the calculated steam generator pressure.

Figure 12 presents the steam generator downcomer levels. The levels decreased rapidly when the feedwater was shut off because the liquid was redistributed from the downcomer to the boiler region. The levels then increased slowly as the EFW was injected. The rate of the level increase in the calculation indicated that too much EFW was being injected during most of the transient. The level decrease in the data at about 300 s could have been caused by a temporary reduction in the EFW flow or a mass redistribution between the downcomer and the riser. The fact that the increase in the data was smooth around 600 s indicated that the pressure increase at that time was a result of reduced steam flow rather than reduced feedwater flow.

In general, the trends of the data and the calculated values were the same, but the calculated values were high (except for the steam generator levels). The calculated results were consistent with the data; that is, if the calculated steam generator pressure had been lower, the primary temperature would have been lower, which would have reduced the pressurizer pressure and level. Since the trend of the steam generator pressure data indicated something was not modeled correctly, this was the focus of the main sensitivity studies.

Basically, there are two methods of reducing the steam generator pressure. One is to release more steam, and the other is to condense more

steam. The former could be accomplished through any of the connections to the main steam lines, while the latter could be accomplished by providing more feedwater or colder feedwater.

The first set of sensitivity calculations involved adjustments to components that, as originally modeled, may not have reflected as-built conditions. The EFW flow was increased 10% for the first 300 s of the transient. This did not affect the secondary pressure very much, so steam release paths were investigated. The steam line relief valve reseal pressure was reduced from 7.536 MPa (1093 psia) to 7.240 MPa (1050 psia), but again this had little effect on the long term pressure behavior. Since altering the existing flows into and out of the steam generator secondary did not significantly affect the response, it was assumed that the atmospheric dump valves were used. This assumption is also consistent with the steam generator pressure slope changes at 300 and 600 s. The leveling off of the pressure at about 300 s could have been caused by the throttling an open dump valve, while the pressure increase starting at 600 s could have been the result of closing an open dump valve.

Several sensitivity calculations were then performed involving adjustments in the atmospheric dump valve operation. First, the steam dump and bypass control system (SDBCS) was used. Figure 13 shows the steam generator pressure response from this calculation, the base calculation, and the data. The dump valves (one in each steam line) opened at about 20 s, causing a rapid depressurization until the valves closed at approximately 85 s. The steam generators depressurized far below the data, resulting in primary system parameters (pressure, temperature, pressurizer level) that were also too low. This indicates that either the available information was not sufficient to model the control system correctly or the dump valves were controlled manually instead of automatically.

The dump valves were then opened various amounts, beginning when the relief valves lifted (about 5 s). Figure 14 shows the steam generator pressure from two cases that bounded the data. The pressure decreased too quickly when the dump valves were 10% open. The calculated depressurization rate was generally good in the case in which the valve was 5% open until 100 s, then was throttled to 3% open.

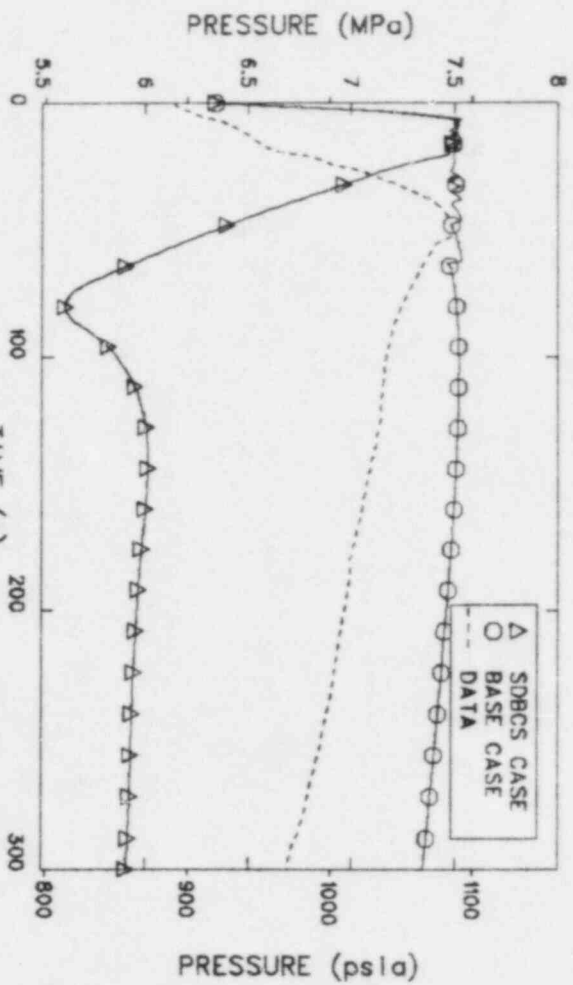


Figure 13. Steam generator A pressure from the SDBCS case, the base case, and the plant data.

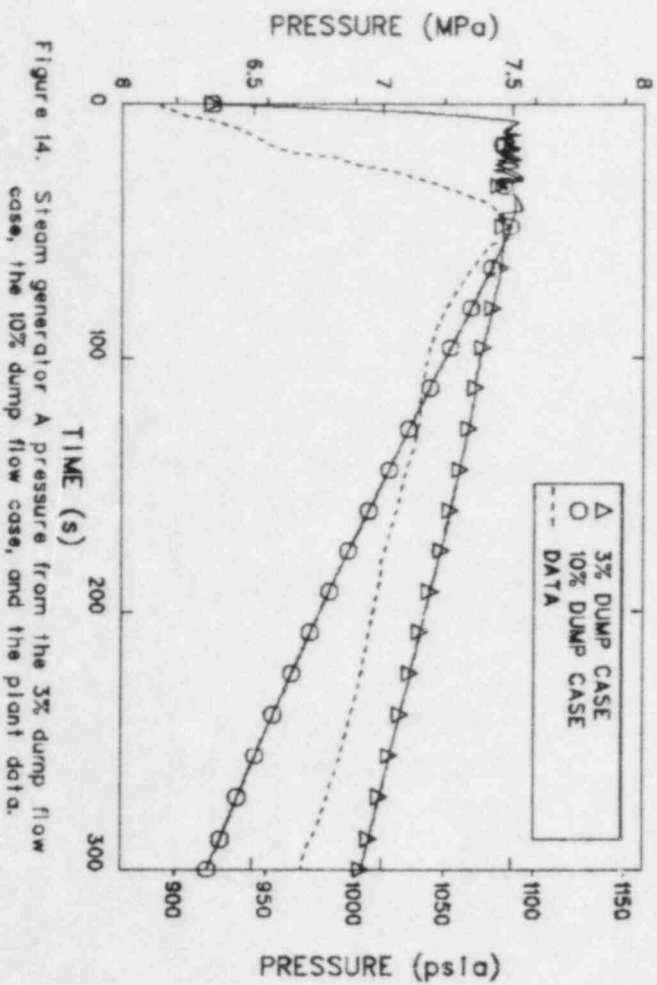


Figure 14. Steam generator A pressure from the 3% dump flow case, the 10% dump flow case, and the plant data.



At this point, rather than trying to operate the dump valves to match the measured steam generator pressure, the measured steam generator pressure was used as a boundary condition for the calculation. Steam was allowed to pass through one dump valve in order to match the calculated steam generator pressure with the measured data. This allowed an evaluation of the primary system parameters for the given secondary system conditions. Comparisons of major parameters from this controlled secondary pressure case, the base case, and the measured data are presented in Figures 15 through 21.

The pressurizer pressures are compared in Figure 15. In the controlled steam generator pressure case, the pressure was too low through most of the transient. The trend of the curve was also not as good as in the base calculation. This difference will be discussed later. Figure 16 presents a comparison of the pressurizer levels. Again, the trend in the controlled pressure case was not very good, although the magnitudes agreed fairly well through most of the transient. The slope changes in the pressurizer pressure and level between 600 and 700 s in the controlled pressure case were caused by the increases in the steam generator pressures starting near 600 s. The increasing steam generator temperature caused the primary system average temperature rate of decrease to slow down. The slower shrink of the reactor coolant, coupled with no change in the CVCS operation, caused the calculated pressurizer level and pressure to increase at a faster rate. Since this change was not seen in the data, it is believed that the operators changed the CVCS operation to reduce the net inflow to the reactor coolant system at this time. Both the pressurizer pressure and level calculations could have been improved by reducing the net CVCS flow into the system at 600 s.

Figure 17 presents a steam generator pressure comparison. The difference in pressure between the controlled pressure case and the data in the first 100 s was caused by the fact that the pressure was controlled through only one dump valve in the calculation. This shows that the MSIVs probably did not close as early as it was assumed. The pressure decrease at about 55 s was probably caused by an atmospheric dump valve opening. The slope change in the steam generator pressure near 300 s could have been

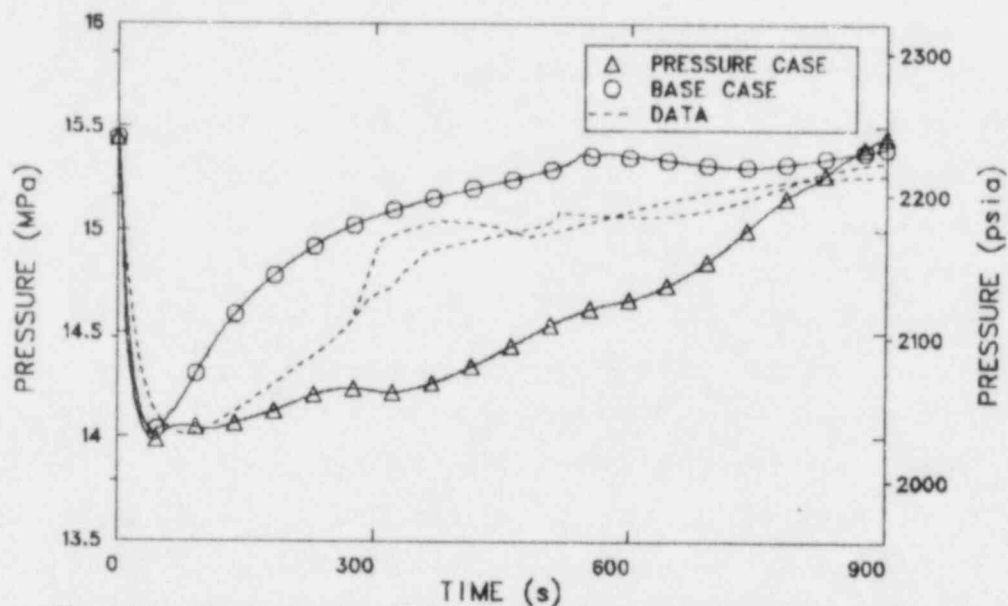


Figure 15. Pressurizer pressure from the controlled pressure case, the base case, and the plant data.

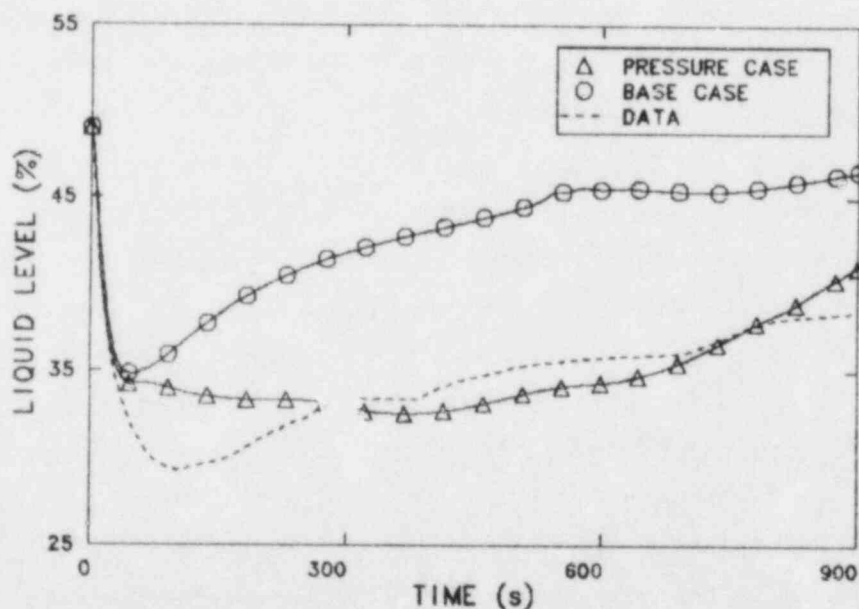


Figure 16. Pressurizer liquid level from the controlled pressure case, the base case, and the plant data.

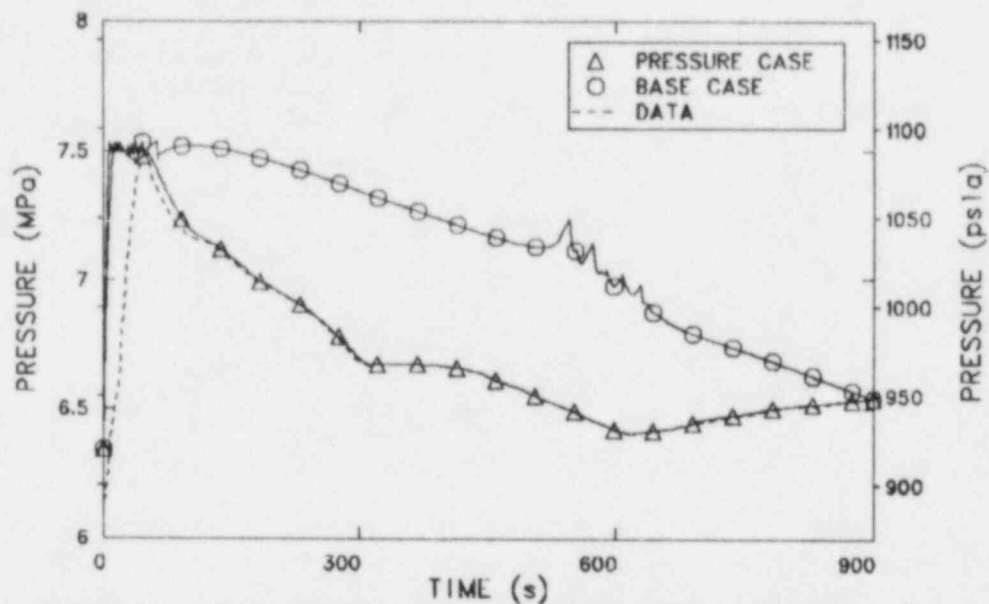


Figure 17. Steam generator A pressure from the controlled pressure case, the base case, and the plant data.

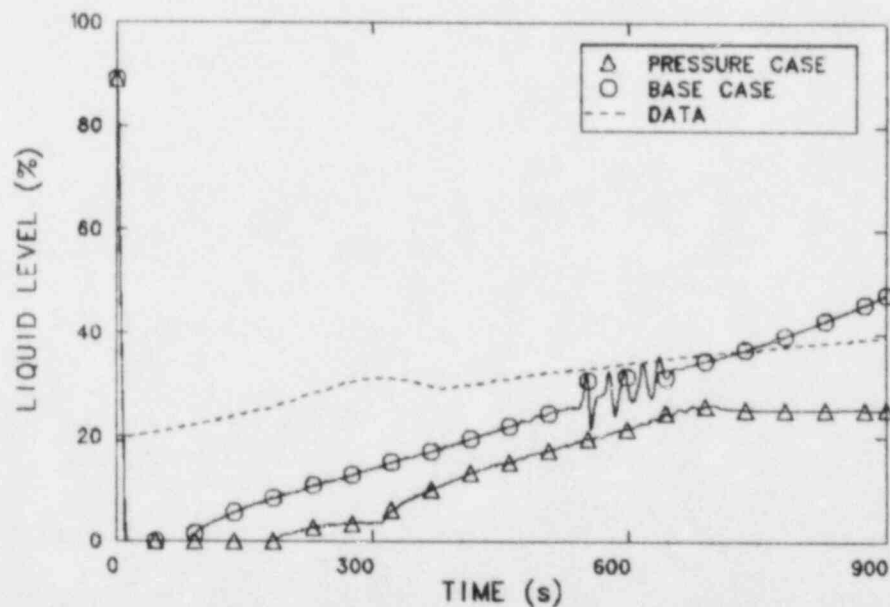


Figure 18. Steam generator A narrow range liquid level from the controlled pressure case, the base case, and the plant data.

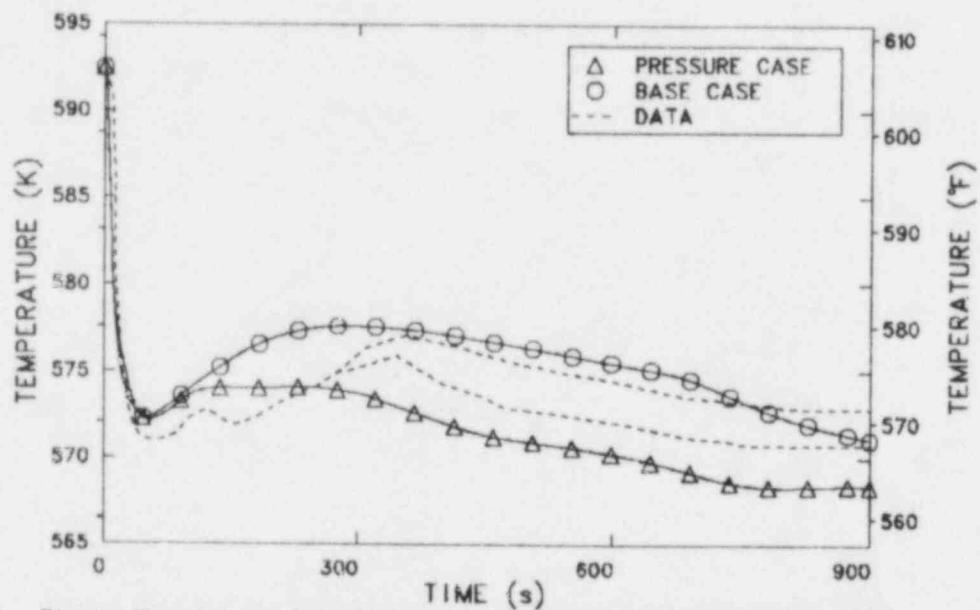


Figure 19. Hot leg temperature from the controlled pressure case, the base case, and the plant data.

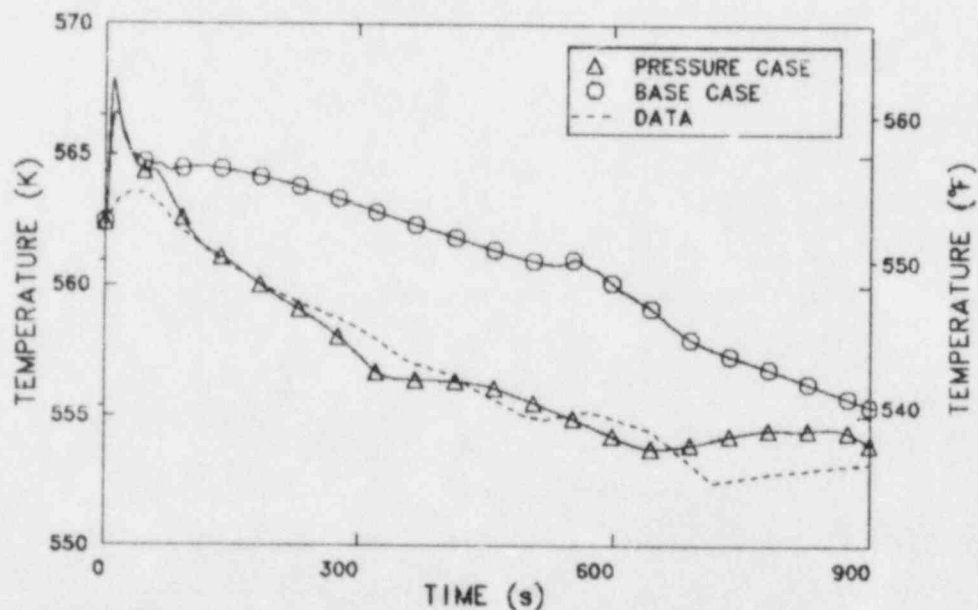


Figure 20. Cold leg temperature from the controlled pressure case, the base case, and the plant data.

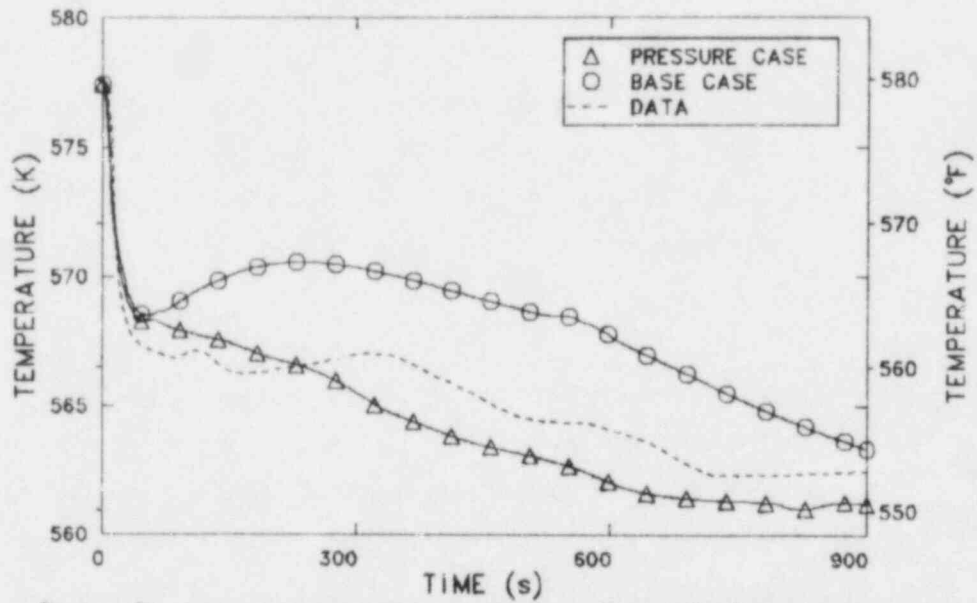


Figure 21. Loop average temperature from the controlled pressure case, the base case, and the plant data.

caused by the partial closing of the valve, and the repressurization starting at 600 s corresponded to the valve being closed.

A steam generator level comparison is presented in Figure 18. The rate of the level increase between 300 and 700 s was greater in the calculations than in the data, indicating the EFW pumps may not have been delivering full rated flow. The steady level in the controlled pressure case after 700 s was caused by code problems related to the condensation model.

Hot leg temperatures from the controlled pressure and base cases are compared with the data in Figure 19. In the controlled pressure case, the temperature rise associated with the flow coastdown (50 to 300 s) was not as great as in the data or the base case. The trend through the rest of the transient was good.

Figure 20 presents a comparison of the cold leg temperatures. The initial temperature increase was not as large as in the base case, although both calculations were higher than the data. There was good agreement between the controlled pressure case and the data through most of the transient.

The loop average temperatures are compared in Figure 21. While the controlled pressure case was closer to the data than the base case, the difference in trend between the controlled pressure case and the data from 50 to 350 s is significant, and can explain the trend differences seen in the pressurizer pressure and level. In the plant data, the average temperature increased during the time that natural circulation was being established (100-300 s), while in the calculation it decreased. The increase in the average temperature caused the liquid to expand, which together with CVCS injection caused the pressurizer level to increase. The increasing level compressed the vapor, causing the pressure to increase.

Thus, by changing the average temperature, the correct pressure and level response should be obtained. Since the secondary system pressure was already controlled, some parameter in the primary coolant system should



have been responsible for the differences between the calculated and measured average temperatures. The reactor coolant pump coastdown was believed to be the most likely cause of the differences.

A constant friction torque term of 2530 N•m (1866 ft•lbf) was added to the modeled pumps. This value was taken from CESSAR 80 pump information since no information on the ANO-2 pumps was available. The transient was calculated again with the steam generator pressure controlled. The addition of the friction torque resulted in a faster pump coastdown. The effect of the pump friction on the transient is shown in Figures 22 through 25.

The hot leg flows from the controlled pressure cases with and without pump friction are shown in Figure 22. It can be seen that adding a pump friction term reduced the pump coastdown time from about 400 s to about 80 s.

Figure 23 shows the loop average temperature from the pump friction calculation compared with the data and the controlled pressure case without pump friction. The faster coastdown caused a large increase in the average temperature between 50 and 150 s. This in turn caused increases in the pressurizer pressure and level, shown in Figures 24 and 25, respectively, that occurred earlier than the increases in the data. This indicated that a pump coastdown rate between the two calculated here may yield better agreement with the measured primary system response. The results illustrated that the primary system behavior was sensitive to the pump coastdown.

### 3.2 Natural Circulation

In the base and controlled pressure calculations, fully developed natural circulation was established by 400 s, when the pump head dropped below zero, indicating that the flow was moving the impeller rather than vice versa. In the pump friction case, natural circulation was fully developed by 100 s. In all the calculations, the mass flow rate remained relatively constant after natural circulation was fully established.

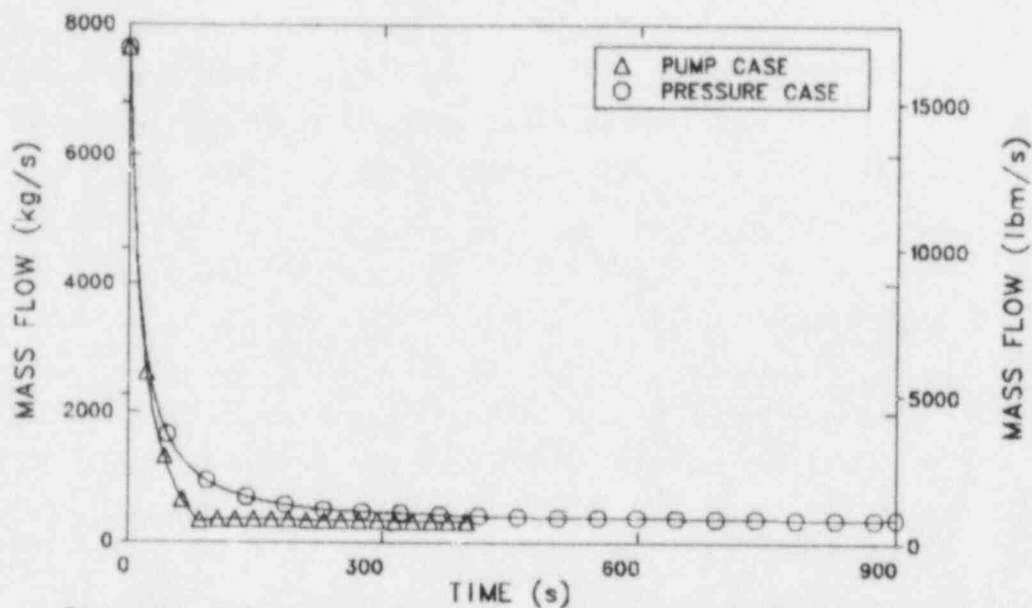


Figure 22. Hot leg mass flow rate from the pump friction case and the controlled pressure case.

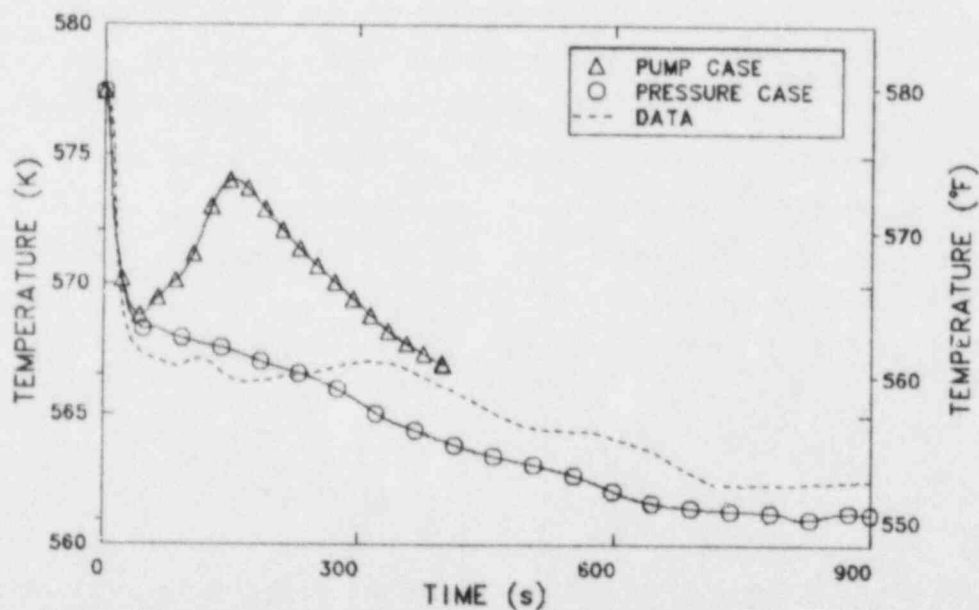


Figure 23. Loop average temperature from the pump friction case, the controlled pressure case, and the plant data.

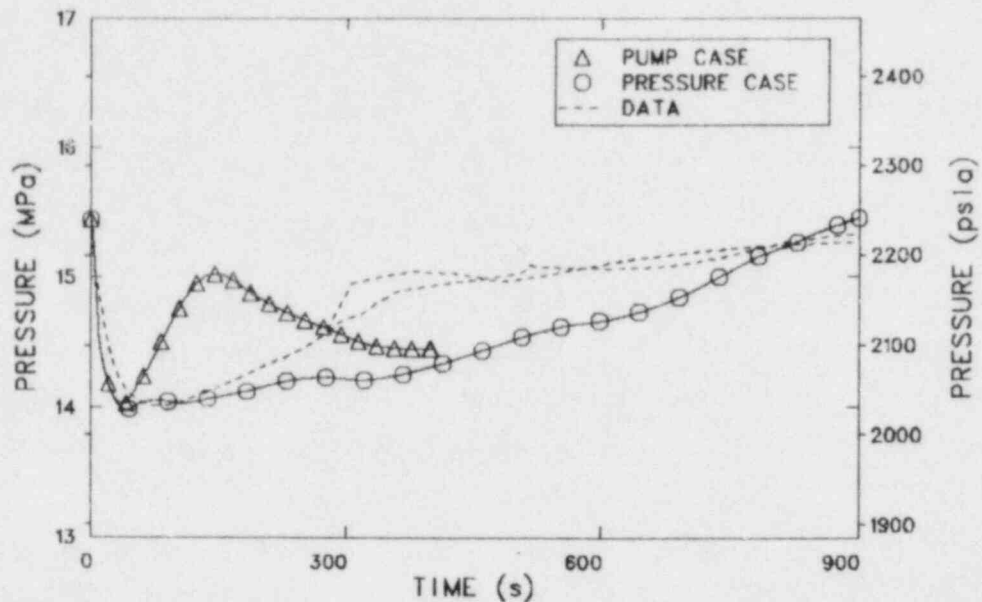


Figure 24. Pressurizer pressure from the pump friction case, the controlled pressure case, and the plant data.

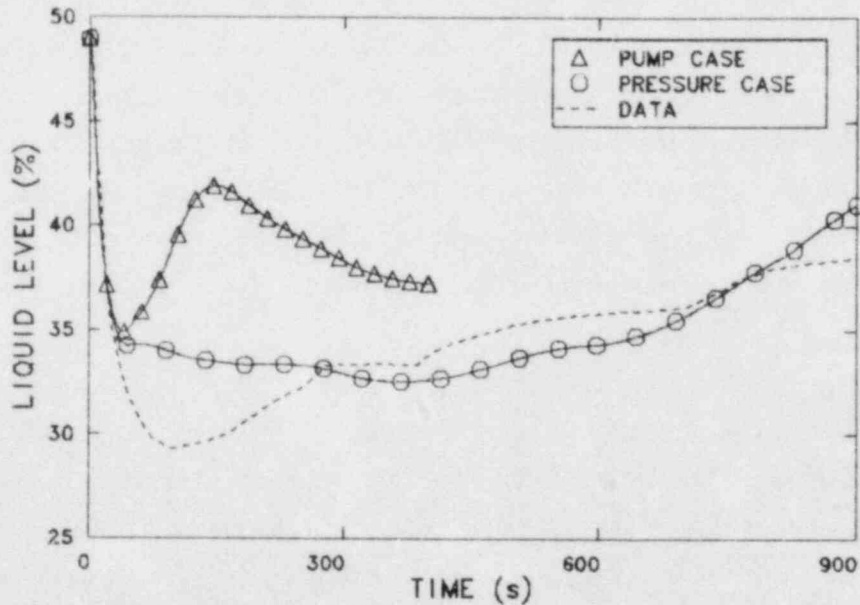


Figure 25. Pressurizer liquid level from the pump friction case, the controlled pressure case, and the plant data.

The hot leg mass flow rates from four different calculations are presented in Figure 26. The fact that the flow was the same for the base case, controlled pressure case, and SDBCS case, despite the widely varying secondary system responses, indicated that as long as the heat sink was available, the same steady natural circulation flow would be established regardless of the steam generator behavior. When the friction torque was added to the pump model, the flow coasted down much faster, and a steady natural circulation flow rate was established at a slightly lower value than in the other cases.

Mass flow rates in the range of 4 to 5% of normal operating flow, as were calculated in natural circulation, are not normally within the measurement range of plant flow instrumentation. Therefore other measurements that are available need to be examined to determine the presence of natural circulation cooling.

One indication of loop flow was the coupling between the cold leg temperature and the steam generator secondary temperature. Figure 27 shows these two temperatures from the controlled pressure calculation. It can be seen that the cold leg temperature was within about 1 K (1.8°F) of the steam generator saturation temperature through most of the transient. The flow rate was low enough that the liquid passing through the steam generator tubes was cooled nearly to the secondary side temperature. Figure 28 shows the corresponding temperatures from the transient data. Again there was good agreement between the two, given the uncertainty in the measurements and the digitization.

The loop flow was also reflected in the loop temperature difference; that is, the difference between the hot and cold leg temperatures in a given loop. Figure 29 presents the loop temperature difference from the base case, the controlled pressure case, and the data. Three phases of loop flow are reflected in this figure. From the transient initiation until about 50 s, the plant was in forced convection cooling. The core power decreased more rapidly than the flow, so the loop temperature difference also decreased. As the flow coastdown continued and the core power decay slowed, the liquid passing through the core began to heat up more, increasing the hot leg temperature and the loop temperature

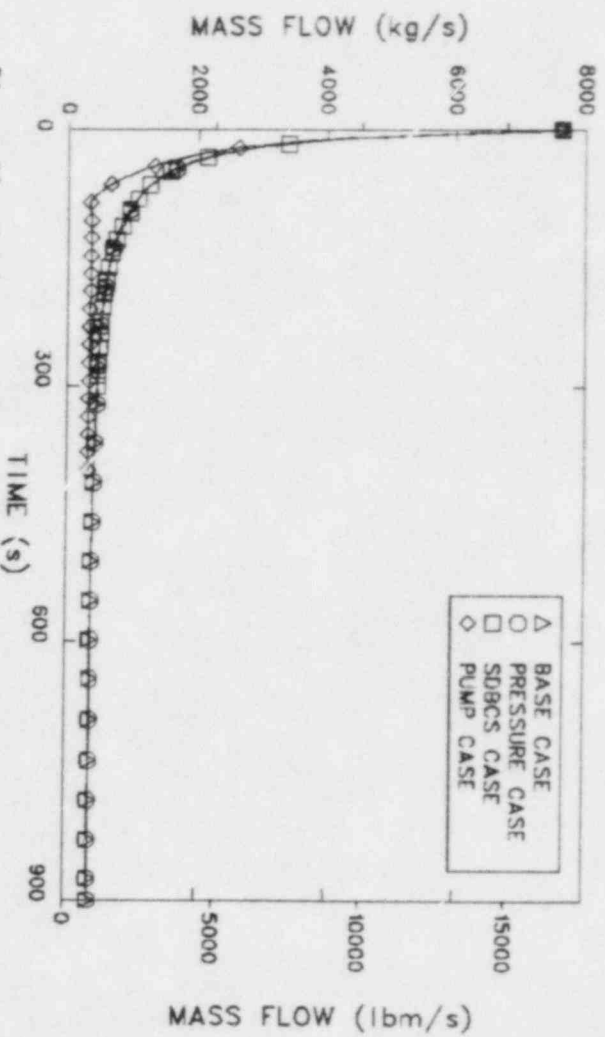


Figure 26. Hot leg mass flow rate from the base case, the controlled pressure case, the SDBCS case, and the pump friction case.

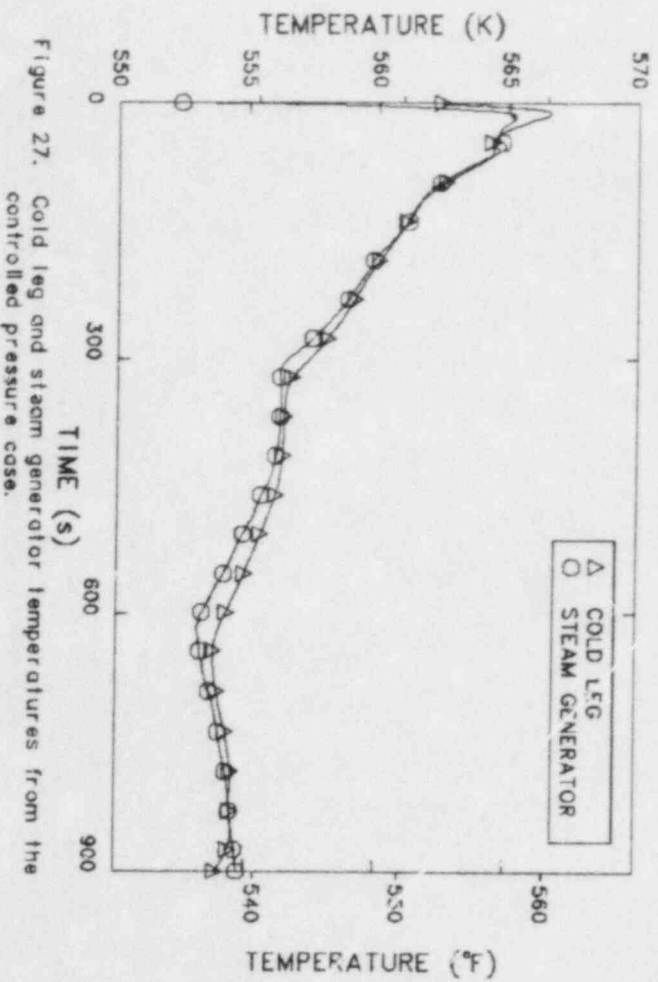
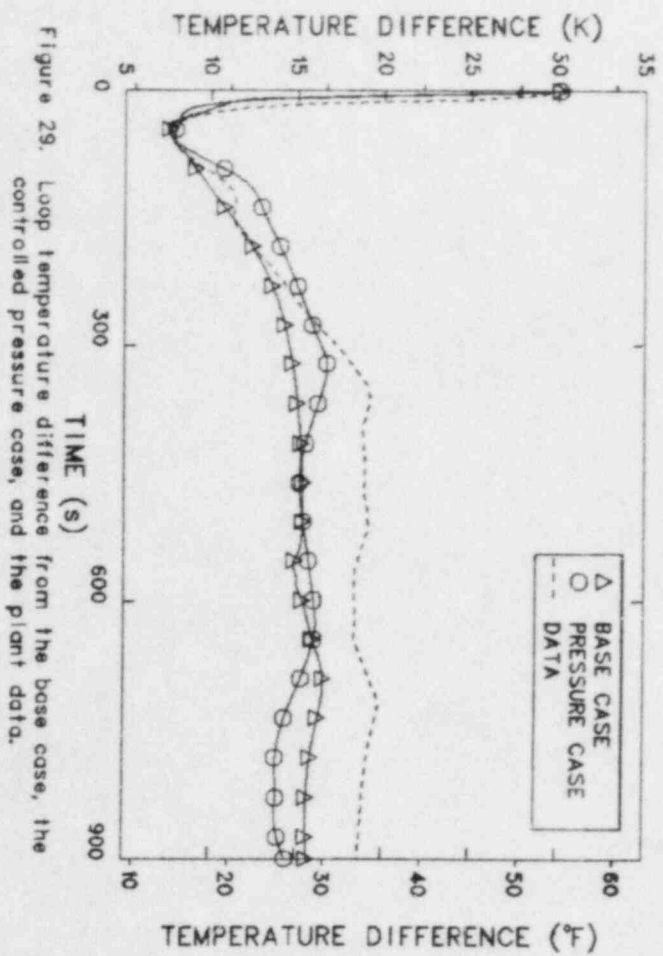
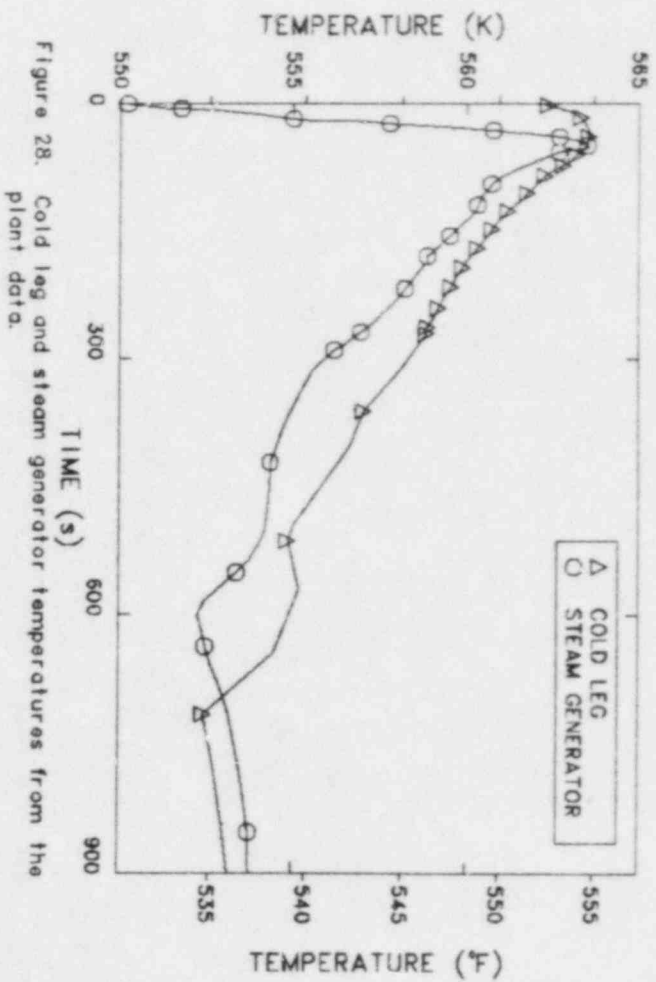


Figure 27. Cold leg and steam generator temperatures from the controlled pressure case.





difference. The loop temperature difference continued to increase until it reached a fairly constant value around 350 to 400 s. As mentioned above, fully developed natural circulation flow was present by 400 s. The increasing temperature difference was an indication of the transition from forced convection to natural circulation, while the constant temperature difference indicated natural circulation was fully established.

The oscillations in the loop temperature difference around the average value during fully developed natural circulation were caused by changes in the steam generator temperature coupled with the loop transit time. For example, in the controlled pressure case, the steam generator pressure increased near 600 s. This caused an increase in the cold leg temperature, which was reflected as a reduction in the loop temperature difference. As this warmer fluid reached the core it was heated above the hot leg temperature at that time. When this hotter fluid reached the hot leg temperature measurement location, the loop temperature difference increased back to the steady state value. The transit time for the fluid to pass from the measurement location in the cold leg to that in the hot leg was about 100 s in this calculation during fully developed natural circulation. The total loop transit time was about 170 s.

The loop temperature difference behavior can be affected by the pump and steam generator secondary behavior. Figure 30 presents the temperature difference from the pump friction and SDBCS cases, as well as from the base case, controlled pressure case, and data.

The increased pump friction caused a faster flow coastdown, which resulted in a larger, more rapid increase in the loop temperature difference. The pump coastdown was complete and natural circulation established by 100 s. The increased flow resistance caused by the pump friction in this calculation resulted in a lower mass flow rate. This meant the loop transit time was increased, so that by 100 s the steady state natural circulation loop temperature difference had not yet been established, although the steady flow rate had been established. The decrease in the loop temperature difference between 150 and 400 s was caused by the core power decay.

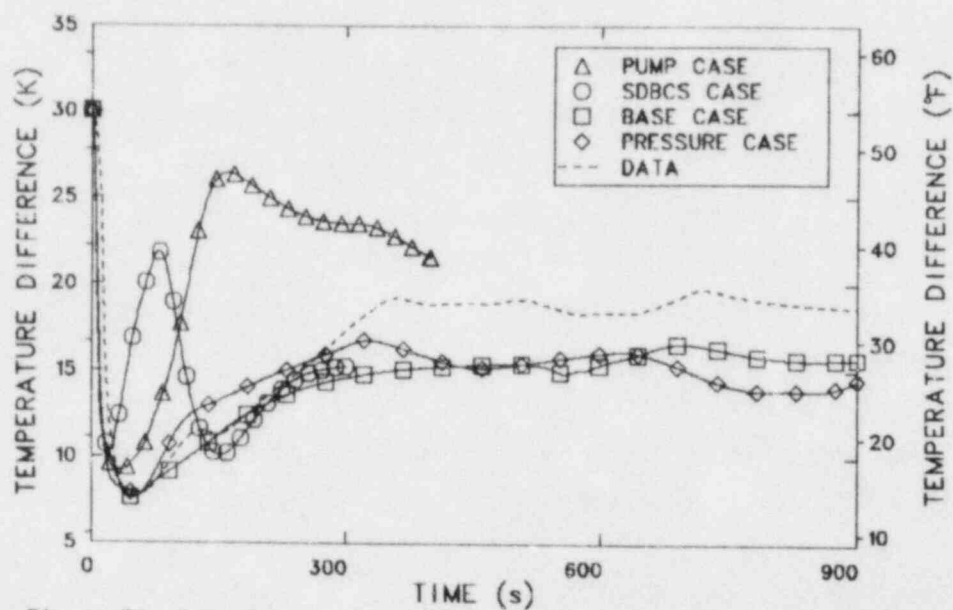


Figure 30. Loop temperature difference from the pump friction case, the SDBCS case, the base case, the controlled pressure case, and the plant data.

The effect of the steam generator pressure (temperature) on the loop temperature difference was shown in the SDBCS case. When the atmospheric dump valves opened at about 20 s, the steam generator pressure decreased rapidly, as did the cold leg temperature. This caused a sharp increase in the temperature difference. As the colder fluid reached the hot leg, the temperature difference decreased again. After the dump valves closed at about 85 s, the secondary pressure remained fairly constant. The loop temperature difference was then comparable to that in the base and controlled pressure calculations. This indicated that the loop temperature difference and flow rate in steady, fully developed natural circulation flow were determined by the core power and the loop flow resistance; the temperature of the heat sink was not significant. A changing steam generator temperature did, however, have a transient effect on the temperature difference, as described above.

#### 4. CONCLUSIONS

Conclusions drawn from the analysis of the June 24, 1980 LOSP transient at ANO-2 are presented below.

Modeling the plant using only the operational information provided in Reference 2 was not sufficient to explain the plant transient response. The differences between the plant data and the calculations showed that some systems were controlled manually rather than automatically.

The operators manually controlled the atmospheric dump valves and the CVCS during the transient. The atmospheric dump valves upstream of the MSIVs opened by 55 s to reduce the steam generator pressure, then were closed near 600 s. These operations were seen in the steam generator pressure slope differences between the base calculation and the data. The CVCS was controlled manually by 500 s to increase the pressurizer level above the programmed setpoint. This operation was shown by the plant strip chart data. The CVCS operation was changed again near 600 s to slow the pressurizer pressure and level increases. The controlled pressure sensitivity calculation showed that the net CVCS inflow to the primary system had to be reduced at this time to compensate for the closing of the atmospheric dump valves.

The reactor coolant system response was sensitive to the steam generator secondary behavior. The steam generator temperature affected the primary system hot and cold leg temperatures. The cold leg temperature was close to the steam generator temperature through most of the transient. Since the pressurizer level and pressure were sensitive to the average temperature, they were indirectly affected by the steam generator pressure.

The reactor coolant system response was very sensitive to the flow coastdown rate. In the pump friction sensitivity calculation, the faster flow coastdown caused larger and earlier increases in the hot leg and average temperatures. This in turn caused the pressurizer level and pressure to increase faster in the calculation than in the data.

The core power and loop flow resistance determined the steady loop temperature difference and the mass flow rate in fully developed natural circulation. While the secondary coolant system did affect the loop temperatures, it did not affect the mass flow rate and had only a transient effect on the steady loop temperature difference. Natural circulation was present in each of the calculations performed, and was fully developed (no positive pump work) by 400 s.

The presence of natural circulation was evident in the plant temperature response. This was important because natural circulation flow rates are generally not within the measurement range of plant loop flow instruments. When natural circulation was present, the cold leg temperature was very close to the steam generator secondary temperature. An indication of fully developed natural circulation was a fairly constant loop temperature difference while the hot and cold leg temperatures were changing. Perturbations in the loop temperature difference were seen as the steam generator pressure changed, but the temperature difference returned to the steady value as the warmer or cooler fluid passed through the coolant loop. The loop temperature difference also slowly increased during the transition from forced convection to natural circulation cooling, although this indication could be clouded by transients in the steam generator pressure.

## 5. REFERENCES

1. V. H. Ransom et al., RELAP5/MOD1.5: Models, Developmental Assessment, and User Information, October 1982, EGG-NSMD-6035.
2. R. A. Pendergraft, Preliminary Unit Transient Report, Report No. 2-80-20, June 1980, Arkansas Power and Light Company.
3. Arkansas Power and Light Company, Arkansas Nuclear One, Unit 2, License Application FSAR, March 1974, Docket-50368-63.



<b>NRC FORM 335</b> <small>(11-81)</small>		<b>U.S. NUCLEAR REGULATORY COMMISSION</b> <b>BIBLIOGRAPHIC DATA SHEET</b>		<b>1. REPORT NUMBER (Assigned by DDC)</b> EGG-NTAP-6309	
<b>4. TITLE AND SUBTITLE</b> Analysis of the June 24, 1980 Loss of Off-Site Power Transient at Arkansas Nuclear One Unit 2				<b>2. (Leave blank)</b>	
<b>7. AUTHOR(S)</b> Paul D. Bayless				<b>3. RECIPIENT'S ACCESSION NO.</b>	
<b>9. PERFORMING ORGANIZATION NAME AND MAILING ADDRESS (Include Zip Code)</b> EG&G Idaho, Inc. Idaho Falls, ID 83415				<b>5. DATE REPORT COMPLETED</b> MONTH: September YEAR: 1983	
<b>12. SPONSORING ORGANIZATION NAME AND MAILING ADDRESS (Include Zip Code)</b> Office for Analysis and Evaluation of Operational Data U.S. Nuclear Regulatory Commission Washington, DC 20555				<b>DATE REPORT ISSUED</b> MONTH: September YEAR: 1983	
				<b>6. (Leave blank)</b>	
				<b>8. (Leave blank)</b>	
				<b>10. PROJECT/TASK/WORK UNIT NO.</b>	
				<b>11. FIN NO.</b> A6234	
<b>13. TYPE OF REPORT</b> Technical Report			<b>PERIOD COVERED (Inclusive dates)</b>		
<b>15. SUPPLEMENTARY NOTES</b>				<b>14. (Leave blank)</b>	
<b>16. ABSTRACT (200 words or less)</b> <p>The June 24, 1980 loss of off-site power transient at Arkansas Nuclear One Unit 2 was analyzed using the RELAP5 computer code. The transient was investigated to understand the overall plant response, particularly in relation to natural circulation cooling. Sensitivity calculations were performed to identify operator actions that may have been taken during the transient. The effect of the various sensitivity calculations on natural circulation was examined. Methods of identifying the presence of natural circulation cooling were investigated.</p>					
<b>17. KEY WORDS AND DOCUMENT ANALYSIS</b>			<b>17a. DESCRIPTORS</b>		
<b>17b. IDENTIFIERS/OPEN-ENDED TERMS</b>					
<b>18. AVAILABILITY STATEMENT</b> Unlimited			<b>19. SECURITY CLASS (This report)</b> Unclassified		<b>21. NO. OF PAGES</b>
			<b>20. SECURITY CLASS (This page)</b> Unclassified		<b>22. PRICE</b> \$